

# Long noncoding RNA FTX is upregulated in gliomas and promotes proliferation and invasion of glioma cells by negatively regulating miR-342-3p

Weiguang Zhang<sup>1,7</sup>, Yunke Bi<sup>2,7</sup>, Jianhua Li<sup>1,7</sup>, Fei Peng<sup>3,7</sup>, Hui Li<sup>4</sup>, Chenguang Li<sup>5</sup>, Laizang Wang<sup>1</sup>, Fubin Ren<sup>1</sup>, Chen Xie<sup>1</sup>, Pengwei Wang<sup>6</sup>, Weiwei Liang<sup>6</sup>, Zhi Wang<sup>1</sup> and Dan Zhu<sup>6</sup>

Gliomas remain a major public health challenge, posing a high risk for brain tumor-related morbidity and mortality. However, the mechanisms that drive the development of gliomas remain largely unknown. Emerging evidence has shown that long noncoding RNAs are key factors in glioma pathogenesis. qRT-PCR analysis was used to assess the expression of FTX and miR-342-3p in the different stages of gliomas in tissues. Bioinformatics tool DIANA and TargetScan were used to predict the targets of FTX and miR-342-3p, respectively. Pearson's correlation analysis was performed to test the correlation between the expression levels of FTX, miR-342-3p, and astrocyte-elevated gene-1 (AEG-1). To examine the role of FTX in regulating proliferation and invasion of glioma cells, specific siRNA was used to knockdown FTX, and MTT (3-(4,5-dimethylthiazol-2-yl)-2,5-diphenyltetrazolium bromide) and transwell assays were performed. Furthermore, rescue experiments were performed to further confirm the regulation of miR-342-3p by FTX. We then found that the expression of FTX and miR-342-3p was associated with progression of gliomas. FTX directly inhibited the expression of miR-342-3p, which subsequently regulates the expression of AEG-1. Collectively, FTX is critical for proliferation and invasion of glioma cells by regulating miR-342-3p and AEG-1. Our findings indicate that FTX and miR-342-3p may serve as a biomarker of glioma diagnosis, and offer potential novel therapeutic targets of treatment of gliomas.

*Laboratory Investigation* (2017) **97**, 447–457; doi:10.1038/labinvest.2016.152; published online 23 January 2017

Gliomas account for almost 80% of primary malignant brain tumors, which cause ~13 000 deaths annually in the United States.<sup>1,2</sup> Gliomas encompass all the tumors that originate from glial cells, including astrocytic tumors (grades I (pilocytic astrocytoma), II (astrocytoma), III (anaplastic astrocytoma), and IV (glioblastoma or GM)), oligodendrogliomas, and other mixed gliomas.<sup>3</sup> A histological grading scheme is critical for assessing glioma behavior and determining therapeutic approaches for patients, but does not significantly contribute to understanding the biological mechanisms of glioma progression.<sup>4</sup> Recent studies have revealed several genes associated with glioma development, including epidermal growth factor receptor and isocitrate dehydrogenases, and epigenetic regulation was found to have an important role in glioma progression.<sup>5–7</sup>

Long noncoding RNAs (lncRNAs) are non-protein coding transcripts longer than 200 nucleotides.<sup>8</sup> Global transcriptional analysis and genomewide tiling arrays have shown that the human genome is prevalently transcribed into lncRNAs.<sup>9,10</sup> The most well-characterized function of lncRNAs is acting as epigenetic modulators.<sup>11</sup> In addition, lncRNAs were also reported to have sensory, guiding, and scaffolding capacities.<sup>12</sup> Owing to lncRNA abundance and their multiple functions, they have gained widespread attention in recent years. Studies have shown that lncRNAs are involved in many biological and pathological processes, including stem cell pluripotency and oncogenesis.<sup>13,14</sup> With regard to gliomas, emerging evidence has revealed distinctive lncRNA profiles in low- and high-grade gliomas and in different subtypes of gliomas.<sup>15–17</sup>

<sup>1</sup>Department of Neurosurgery, The Fourth Affiliated Hospital of Harbin Medical University, Harbin, China; <sup>2</sup>Department of Neurosurgery, Shanghai First People's Hospital of Shanghai Jiao Tong University School of Medicine, Shanghai, China; <sup>3</sup>Department of Neurosurgery, The First Affiliated Hospital of Harbin Medical University, Harbin, China; <sup>4</sup>Department of Neurosurgery, The 242 Hospital of Harbin, Harbin, China; <sup>5</sup>Department of Neurosurgery, The Second Affiliated Hospital of Zhejiang University School of Medicine, Hangzhou, China and <sup>6</sup>Department of Neurology, The Second Affiliated Hospital of Harbin Medical University, Harbin, China

Correspondence: Dr D Zhu, MD, PhD, Department of Neurology, The Second Affiliated Hospital of Harbin Medical University, 246 Xuefu Road, Harbin 150086, China. E-mail: zhudan66666@126.com

<sup>7</sup>These authors contributed equally to this work.

Received 15 July 2016; revised 29 November 2016; accepted 1 December 2016

FTX is a highly conserved lncRNA located at the X-chromosome inactivation (XCI) center.<sup>18</sup> FTX escapes XCI in females, and has an X-inactive-specific transcript that is the master regulator of X-inactivation initiation. As evidenced by findings in *FTX*-null mouse ES cells, *FTX* is required for the expression of transcripts within the XCI center, including *Xist*.<sup>18</sup> FTX was also found to be associated with colorectal cancer progression, and to inhibit proliferation and metastasis of hepatocellular carcinoma by binding MCM2 (minichromosome maintenance complex component 2) and miR-374a.<sup>19</sup> However, whether FTX is involved in the development of gliomas and its potential role(s) of regulating glioma progression remain unknown.

In this study, we investigated the expression levels of FTX in different stages of glioma in tissues, and found that siRNA-mediated depletion of FTX inhibited proliferation and invasion of glioma cells *in vitro*. Bioinformatic analysis revealed that FTX directly binds to miR-342-3p, which further targets astrocyte-elevated gene-1 (AEG-1). Rescue experiments were then performed to confirm the promotive effects of the FTX on proliferation and invasion of glioma cells by targeting miR-342-3p.

## MATERIALS AND METHODS

### Human Samples

Tumor specimens were collected from glioma patients who underwent surgery in the Department of Neurosurgery of the Fourth Affiliated Hospital of Harbin Medical University in China between 2012 and 2014. Twenty-two glioma and five normal brain tissue samples were obtained, immediately snap frozen in liquid nitrogen, and stored at  $-80^{\circ}\text{C}$  until analysis. All samples were diagnosed in accordance with the World Health Organization criteria. Written informed consent was obtained from all patients. The study was approved by the Institutional Review Board of Harbin Medical University and the Harbin Medical University Research Ethics Committee. This research was conducted in accordance with the Declaration of Helsinki.

### Quantitative Real-Time-PCR (qRT-PCR)

qRT-PCR was performed as described previously.<sup>20</sup> Briefly, tissue samples were homogenized in TRIzol reagent (Invitrogen, Carlsbad, CA, USA), and RNA was isolated as suggested by the manufacturer. qRT-PCR for miR-342-3p was performed using the TaqMan MicroRNA Assay (Applied Biosystems, Foster City, CA, USA) with 10 ng of total RNA. For mRNA, 1.0  $\mu\text{g}$  of each RNA sample was reverse transcribed to cDNA using SuperScript II Reverse Transcriptase (Invitrogen), followed by qRT-PCR with Fast SYBR Green Master Mix (Applied Biosystems), as described in the manufacturer's protocol. qRT-PCR was performed using an Applied Biosystems 7500 qRT-PCR System with TaqMan Universal. The expression levels of miRNA and each gene were normalized to that of U6 small nuclear RNA or  *$\beta$ -actin* genes, respectively. Relative expression levels between

samples were calculated using the  $2^{-\Delta\Delta\text{CT}}$  method. Primers for *AEG-1* and  *$\beta$ -actin* were as follows: *AEG-1* sense, 5'-ACGACC TGGCCTTGCTGAAGAATCT-3' and antisense, 5'-CGGTT GTAAGTTGCTCGGTGGTAA-3';  *$\beta$ -actin* sense, 5'-TCATG TTTGAGACCTTCAA-3' and antisense, 5'-GTCTTTGCGGA TGTCACG-3'.

### Cell Lines

The human glioma cell lines (U87MG and LN18) and HEK293T cells were cultured in DMEM supplemented with 10% fetal bovine serum (Invitrogen), 25  $\mu\text{g}/\text{ml}$  penicillin, and 25  $\mu\text{g}/\text{ml}$  streptomycin (Invitrogen). All cells were incubated at  $37^{\circ}\text{C}$  in a 5%  $\text{CO}_2$  atmosphere with 90% relative humidity.

### miRNA Mimics, Plasmids, Luciferase Activity and Cellular Transfection

miRNAs and siRNAs were synthesized by Gene Pharma (Shanghai, China). AEG-1 3'-UTRs containing the binding sites and mutant binding sites of miR-342-3p were synthesized and ligated to psiCHECK-2. For the dual luciferase assay, cells were plated in 24-well plates and transiently transfected using Lipofectamine RNAiMAX (Invitrogen) with combinations of miRNA, plasmid, and/or siRNA with the *Renilla* luciferase pRL-CMV construct. Luciferase assays were used to quantitate miRNA binding to the functionally conserved miR-342-3p binding sites in the 3'-UTR of the predicted targets. Functionally conserved miR-342-3p binding sites in 3'-UTRs were identified by decreased luciferase activity. Luciferase activity was measured using a Dual Luciferase Assay Kit (Promega, Madison, WI, USA) and normalized against *Renilla* luciferase activity 48 h after transfection. Luciferase assays were performed 2 days after transfection, using a Dual Luciferase Assay Kit.

### MTT Assay

Cells were seeded at a density of 2000 cells per well into 96-well plates and cultured for 1–4 days after transfection. The cells were then incubated with 0.5 mg/ml of MTT (3-(4,5-dimethylthiazol-2-yl)-2,5-diphenyltetrazolium bromide; Sigma-Aldrich, St Louis, MO, USA) for 4 h according to the manufacturer's instructions. The MTT assay was used to assess cell viability, and was performed according to the manufacturer's protocol (TOX1-1KT; Sigma-Aldrich). Absorbance was measured using a microtiter plate reader at 570 nm.

### Colony Formation Assay

Cells were seeded into 6-well culture plates at a density of 500 cells per well and cultured in a growth medium at  $37^{\circ}\text{C}$  for 2 weeks. The medium was changed every 3 days. Cells were then fixed with 10% formalin, stained with 0.5% crystal violet solution, washed with PBS, and photographed. The colony numbers were determined using the NIH ImageJ software.

### Transwell Assay

A transwell assay was used to measure cell invasion ability. Transfected glioma cells ( $5 \times 10^4$  per well) were cultured in 1% FBS DMEM medium and seeded into the upper chamber of each insert with Matrigel (BD Biosciences, Bedford, MA, USA). The lower chamber of the transwell was then filled with DMEM complete medium. After 12 h, the upper surface of the membrane was wiped with a cotton tip, and cells that attached to the lower surface were stained with crystal violet. The invading cells were photographed and counted in six random fields.

### Western Blot

Total cell lysates were prepared by disrupting cells with RIPA buffer containing protease and phosphatase inhibitor cocktails (Thermo Scientific, Pittsburgh, PA, USA), and centrifuged at maximum speed for 10 min at 4 °C. Protein concentrations were determined using the BCA Protein Assay Reagent (Thermo Scientific). Equal quantities of protein samples were separated by SDS-PAGE and transferred onto nitrocellulose membranes (Bio-Rad, Richmond, CA, USA). Anti-AEG-1 and anti- $\beta$ -actin were purchased from Abcam (Cambridge, MA, USA). HRP-conjugated secondary antibodies (Abcam) were used for primary antibody detection. The bound antibodies were visualized using an ECL Chemiluminescence System (Thermo Scientific).

### Animal Models

We established stable FTX-knockdown U87MG cells and examined the FTX function *in vivo* as described previously.<sup>20</sup> Sixteen male BALB/c nude mice (4 weeks old) were randomly divided into two groups (eight animals per group). U87MG cells ( $2 \times 10^6$ ) were suspended in 200  $\mu$ l PBS and injected subcutaneously into the left flank of each nude mouse. Tumor growth in each group was monitored by taking two-dimensional measurements of tumors from each mouse every 5 days following cell line inoculation. All of the mice were killed on day 25, and the tumors were weighed. All experiments were carried out in accordance with animal research protocols.

### Immunohistochemistry

Immunohistochemistry (IHC) was performed on formalin-fixed, paraffin-embedded mouse subcutaneous tumors. Tissue sections were deparaffinized, rehydrated, and heat-induced antigen retrieval was performed in an autoclave in 10 mM citrate buffer (pH 6.0) for 5 min. Endogenous peroxidase activity was blocked with 0.3% hydrogen peroxide for 15 min. Sections were incubated with anti-AEG-1 at 4 °C overnight. Tissue sections were then incubated with secondary antibody for 30 min and developed using AEC Chromagen (Dako; K346911-2).

### Statistical Analysis

Experimental data are expressed as the mean  $\pm$  s.d. Statistical software (SPSS version 12.0; SPSS, Chicago, IL, USA) was used to perform Student's *t*-tests or one-way analysis of variance.  $P < 0.05$  was considered statistically significant.

## RESULTS

### Upregulated Expression of FTX in Glioma Tissues

To explore the clinical relevance of lncRNA FTX in human gliomas, we analyzed FTX expression in different stages of gliomas in database GDS1962. The results showed over-expression of FTX in all grades of glioma (45 grade II, 31 grade III, and 81 grade IV samples) (Figure 1a). The expression levels of FTX were assayed by qRT-PCR in 22 clinical glioma samples (5 grade II, 6 grade III, and 11 grade IV samples). We consistently observed an increase in FTX expression in all grades of glioma tissues (Figure 1b).

### Knockdown of FTX Inhibited Glioma Cell Proliferation and Invasion

To examine the role of FTX in glioma progression, U87MG and LN18 cells were transfected with FTX siRNA or control siRNA for 2 days. siRNA knockdown efficiency of FTX was confirmed by qRT-PCR (Figure 2a). Cell proliferation was then measured by counting cell numbers at different time points. Cells transfected with FTX siRNA had significantly slower growth rates than those of the control group in both types of glioma cells (Figure 2b). Colony formation showed reduced colony numbers after depletion of FTX (Figure 2c). MTT assays were then performed to further confirm these results. The average OD values at 570 nm were significantly lower in FTX siRNA-transfected cells than in the control mimic-transfected cells (Figure 2d). To analyze the effects of FTX knockdown on glioma cell invasion, we performed transwell cell invasion assays in FTX-knockdown and control glioma cells. As shown in Figure 2e, knockdown of FTX significantly decreased the invasion abilities of glioma cells. We further performed experiments *in vivo*. U87MG cells of stable FTX knockdown were implanted into nude mice subcutaneously. The tumor volume was measured every 5 days after implantation. The tumor growth was significantly reduced after FTX was knocked down (Figure 2f). Subcutaneous tumors were removed subsequently and weighed 25 days after implantation. As shown in Figures 2g and h, silencing of FTX remarkably decreased tumor size and weight.

### miR-342-3p Expression was Directly Regulated by FTX

To explore the mechanism(s) by which FTX regulates glioma cells, the bioinformatics tool DIANA was used to analyze FTX targets,<sup>21</sup> and miR-342-3p was selected as the predicted target with the highest score (Figure 3a). To test this prediction, we first analyzed miR-342-3p expression in 22 clinical examples. In contrast to FTX, expression of miR-342-3p was significantly downregulated in glioma samples (Figure 3b). Pearson's correlation analysis revealed an inverse

correlation between miR-342-3p and FTX in these 22 clinical glioma tissues (Figure 3c). We analyzed miR-342-3p expression in FTX-knockdown glioma cells and found that miR-342-3p was boosted after FTX downregulation (Figure 3d). However, ectopic overexpression of miR-342-3p did not affect FTX expression (Figure 3e).

### miR-342-3p Inhibited Proliferation and Invasion of Glioma Cells

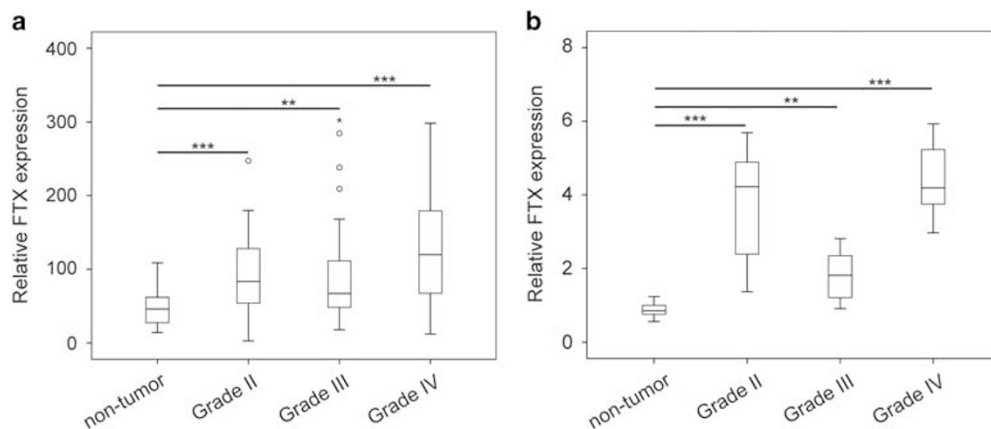
miR-342-3p has been reported to be an anticancer microRNA in multiple types of cancer cells. To determine whether miR-342-3p affects proliferation and invasion of glioma cells, we transfected U87MG and LN18 cells with control mimics miR-342-3p or miR-342-3p inhibitor (miR-342-3p-in), respectively (Figure 4a). While overexpression of miR-342-3p significantly inhibited cell proliferation, inhibition of miR-342-3p promoted cell growth (Figure 4b). Further colony formation and MTT assays were performed to confirm the effects of miR-342-3p on cell proliferation. Transfection of miR-342-3p consistently significantly suppressed cell proliferation, and transfection of miR-342-3p-in enhanced cell proliferation in U87MG and LN18 cells as compared with the control group (Figures 4c and d). Cell invasion ability was determined by transwell assays. As shown in Figure 4e, transfection of miR-342-3p significantly inhibited cell invasion, whereas transfection of miR-342-3p-in significantly increased the number of invading cells.

### Inhibition of miR-342-3p Abrogated the Suppression of Proliferation and Invasion of Glioma Cells Induced by Depletion of FTX

To determine whether FTX exerts biological functions through miR-342-3p, we performed rescue experiments by inhibiting miR-342-3p expression in FTX-knockdown cells (Figure 5a). As shown in Figures 5b–d, proliferation was decreased in FTX-knockdown U87MG and LN18 cells, whereas miR-342-3p-in partially reversed the reduction of proliferation. Furthermore, transwell invasion assays revealed that FTX knockdown significantly inhibited cell invasion, and FTX siRNA transfection with miR-342-3p-in partially rescued the reduction of invading cells (Figure 5e).

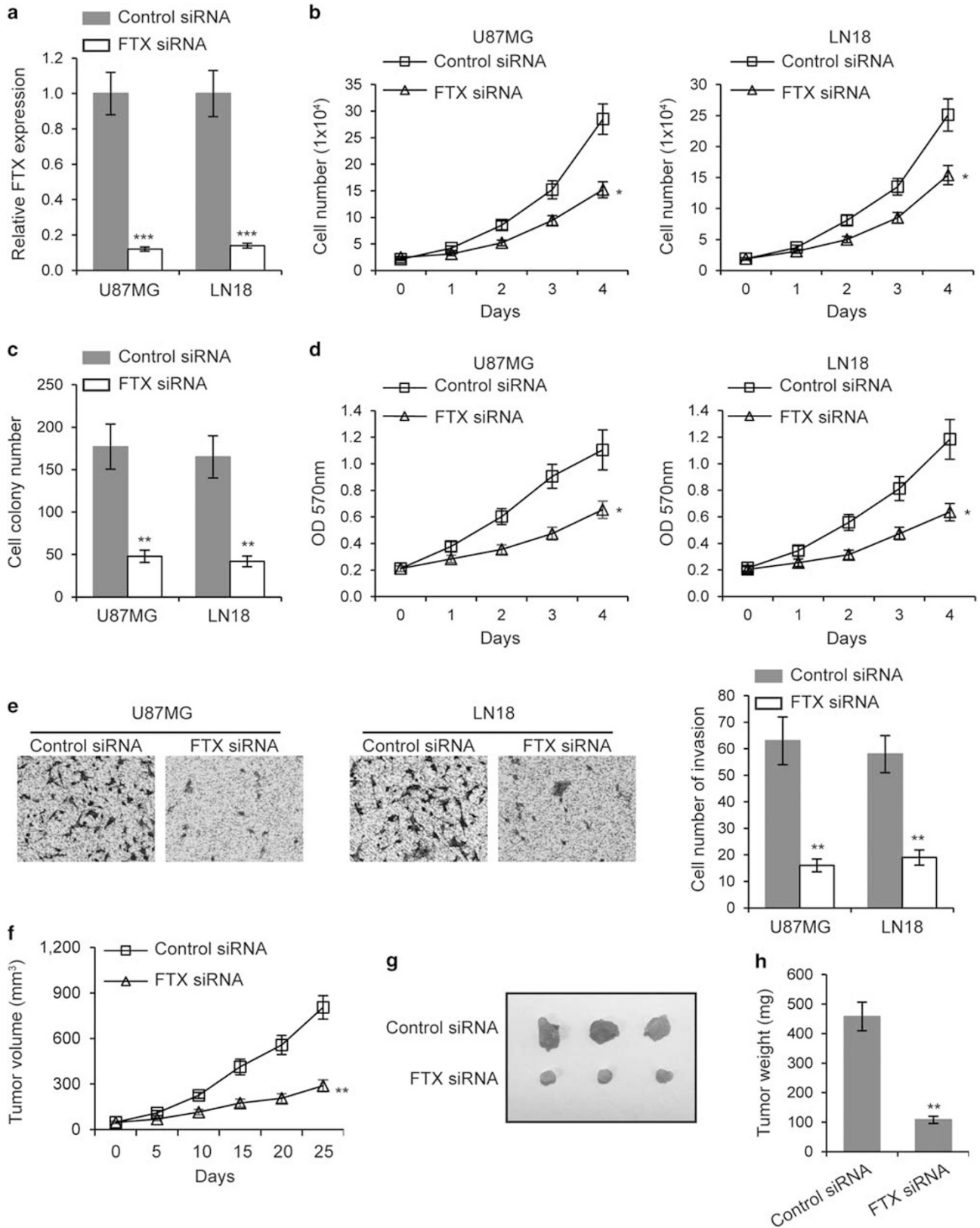
### miR-342-3p Directly Targeted AEG-1

To identify the target of miR-342-3p and understand the mechanisms underlying miR-342-3p function in glioma development, bioinformatics tool TargetScan was used to perform a target search.<sup>22</sup> Since multiple sites of AEG-1 were predicted to bind with miR-342-3p (Figure 6a) and it is a multifunctional mediator in cancer progress,<sup>23</sup> we determined whether AEG-1 is a target of miR-342-3p. U87MG and LN18 cells were transfected for 48 h with control mimics miR-342-3p or miR-342-3p-in, respectively. Western blotting was performed to assess AEG-1 expression. As shown in Figure 6b, we found that miR-342-3p inhibited AEG-1 protein expression, and miR-342-3p-in promoted AEG-1



**Figure 1** Expression of FTX was upregulated in gliomas. (a) FTX expression from GER data set GDS1962 (23 non-tumor, 45 grade II, 31 grade III, and 81 grade IV samples;  $**P < 0.01$ ,  $***P < 0.001$ ). (b) qRT-PCR analysis of FTX expression in 22 clinical glioma tissues (5 grade II, 6 grade III and 11 grade IV) compared with 5 normal brain samples ( $**P < 0.01$ ,  $***P < 0.001$ ).

**Figure 2** Knockdown of FTX inhibited glioma cell proliferation and invasion. (a) FTX expression was determined by qRT-PCR 48 h after control small interfering RNA (siRNA) or FTX siRNA transfection in U87MG and LN18 glioma cells. (b) Cell numbers; (c) colony formation; and (d) MTT (3-(4,5-dimethylthiazol-2-yl)-2,5-diphenyltetrazolium bromide) cell proliferation assays in control siRNA- or FTX siRNA-transfected U87MG and LN18 cell lines. (e) Transwell invasion assays of U87MG and LN18 cells transfected with control siRNA or FTX siRNA (left). Quantification of invading cells (right). Data shown are the mean  $\pm$  s.d. of three independent experiments. (f) U87MG-stable FTX-knockdown cells were subcutaneously implanted into the nude mice. Tumor volume was measured every 5 days. The subcutaneous tumors were taken photos (g) and weighted (h) in both FTX-knockdown and control groups.  $*P < 0.05$ ,  $**P < 0.01$  and  $***P < 0.001$ .



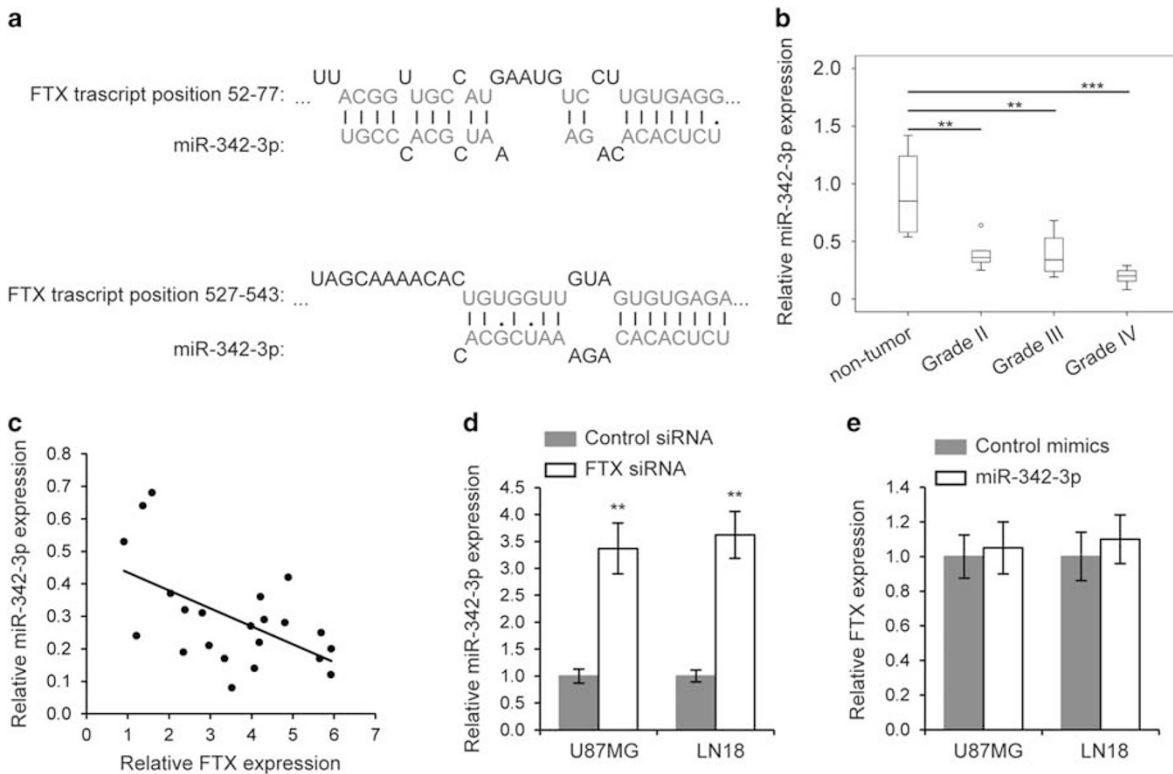


**Figure 3** miR-342-3p expression was determined by FTX. **(a)** The predicted binding sites between FTX and miR-342-3p. **(b)** miR-342-3p expression in 22 clinical glioma tissues (5 grade II, 6 grade III and 11 grade IV) was determined by qRT-PCR and compared with five normal brain samples. **(c)** Pearson's correlation analysis between miR-342-3p and FTX in 22 clinical glioma tissues;  $r = -0.554$ ,  $**P < 0.01$ .  $***P < 0.001$ . **(d)** miR-342-3p expression in FTX-knockdown U87MG and LN18 cells was determined by qRT-PCR. **(e)** FTX expression in control mimics or miR-342-3p-transfected U87MG and LN18 cells was determined by qRT-PCR. Data shown are the mean  $\pm$  s.d. of three independent experiments.  $**P < 0.01$ .

expression. We then constructed the 3'-UTR of AEG-1 with a functionally conserved miR-342-3p binding site, and mutated controls (mut-1 and mut-2) into a pMIR reporter plasmid (Figure 6c). These plasmids were then transfected into HEK293T cells with miR-342-3p. As shown in Figure 6d, miR-342-3p significantly inhibited luciferase activity in wild-type and mutated AEG-1 3'-UTRs, suggesting that miR-342-3p directly targets AEG-1 with multiple binding sites.

### FTX Regulated AEG-1 Expression Through miR-342-3p

To investigate whether FTX functions through AEG-1 mediated by miR-342-3p, we first analyzed the expression of AEG-1 by qRT-PCR in 22 clinical glioma samples. The results showed that expression of AEG-1 was significantly upregulated in gliomas of both low and high grades (Figure 7a). We further analyzed the correlation between AEG-1 and miR-342-3p/FTX. Reverse correlation between AEG-1 and miR-342-3p and positive correlation between AEG-1 and FTX were found in clinical glioma samples (Figures 7b and c). We then performed AEG-1 IHC staining in all glioma specimens and categorized the samples to AEG-1 high and low groups based on the staining levels. We observed increased FTX expression and decreased miR-342-3p expression in high AEG-1 expression group

(Figure 7d). Using mouse subsequent injection model, we observed higher expression of miR-342-3p and lower protein levels of AEG-1 were found in FTX siRNA group (Figure 7e). We next performed western blotting for AEG-1 expression in U87MG and LN18 cells transfected with miR-342-3p and with FTX knockdown. As shown in Figure 7f, knockdown of FTX significantly repressed AEG-1 expression, whereas AEG-1 expression was rescued after introduction of miR-342-3p, demonstrating that the FTX has a pivotal role in glioma progress by regulating miR-342-3p.

### DISCUSSION

Gliomas remain a major public health challenge, posing a high risk for brain tumor-related morbidity and mortality.<sup>1,24</sup> Currently, the mechanisms that drive the development of gliomas are still largely unknown. Exposure to high doses of ionizing radiation and inherited mutations of high-risk genes were the only identified risk factors for developing gliomas.<sup>1,25,26</sup> Recent studies have indicated that targeting specific epigenetic modifications may be a new therapeutic approach for treatment of gliomas.<sup>5</sup> In this study, we found that long noncoding RNA FTX was upregulated during glioma progression. Using bioinformatic analysis and functional studies, we revealed that FTX inhibited expression of

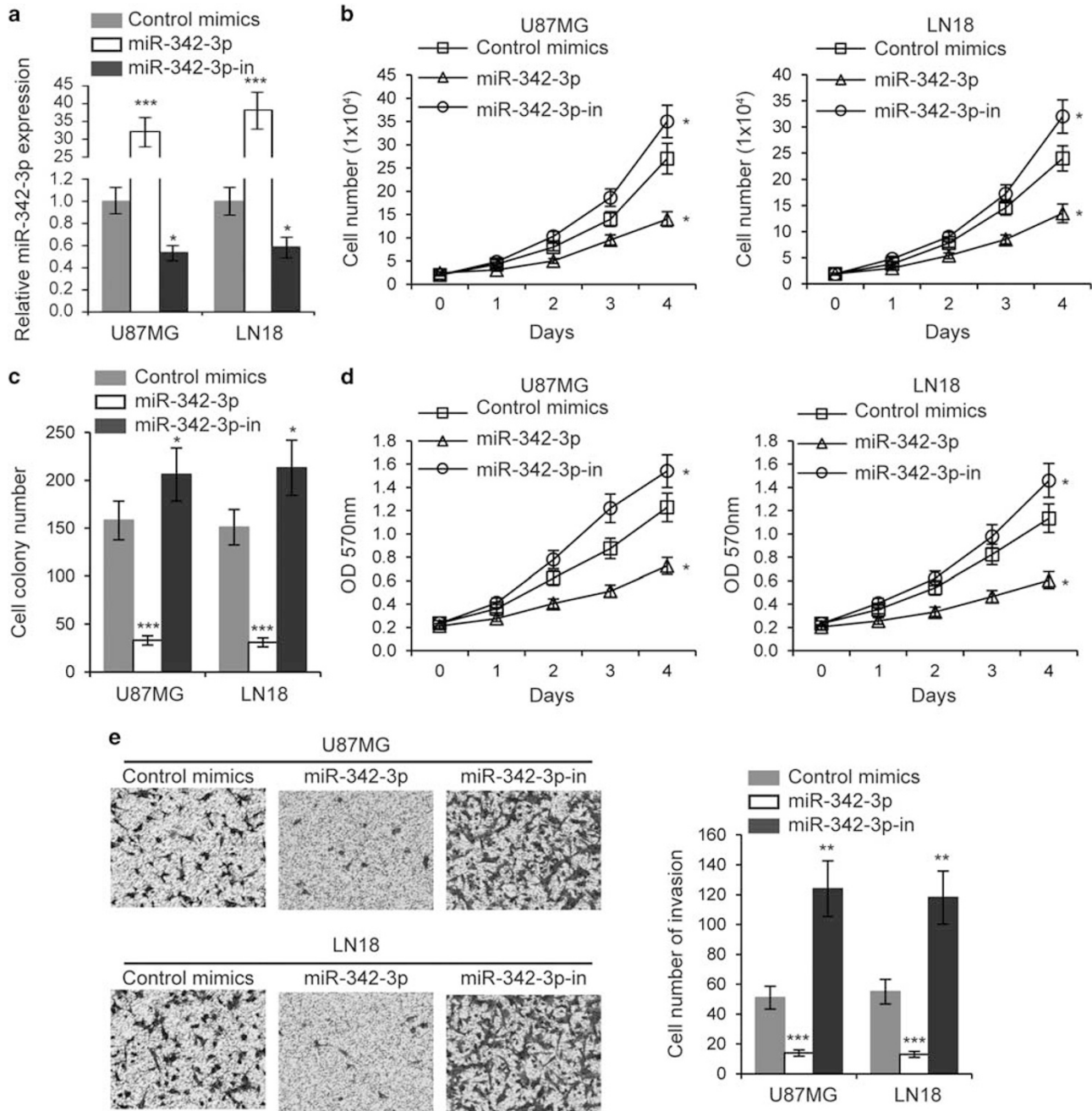


**Figure 4** miR-342-3p inhibited glioma cell proliferation and invasion. (a) miR-342-3p expression was determined by qRT-PCR in U87MG and LN18 cells transfected with control mimics miR-342-3p or miR-342-3p inhibitor (miR-342-3p-in). (b) Cell numbers; (c) colony formation; and (d) MTT (3-(4,5-dimethylthiazol-2-yl)-2,5-diphenyltetrazolium bromide) cell proliferation assays in control mimics miR-342-3p- or miR-342-3p-in-transfected U87MG and LN18 cell lines. (e) Transwell invasion assays of U87MG and LN18 cells transfected with control mimic miR-342-3p or miR-342-3p-in (left). Quantification of invading cells (right). Data shown are the mean  $\pm$  s.d. of three independent experiments. \* $P < 0.05$ , \*\* $P < 0.01$  and \*\*\* $P < 0.001$ .

miR-342-3p, which further targeted AEG-1, thereby promoting proliferation and invasion of glioma cells.

To our knowledge, this is the first study showing that expression levels of FTX have a role in progression of gliomas. lncRNAs are more abundantly expressed in the brain than other regions of the body.<sup>15</sup> Recent emerging evidence has shown that lncRNAs are key factors in

glioma pathogenesis.<sup>15-17</sup> For example, HOX transcript antisense intergenic RNA, a target of oncogene c-Myc, is upregulated during glioma progression and promotes growth and invasion of glioma cells.<sup>27</sup> Maternally expressed gene 3 was associated with prolonged survival of patients with GM multiforme, and is considered to be a tumor suppressor that inhibits mouse double minute 2 homolog,

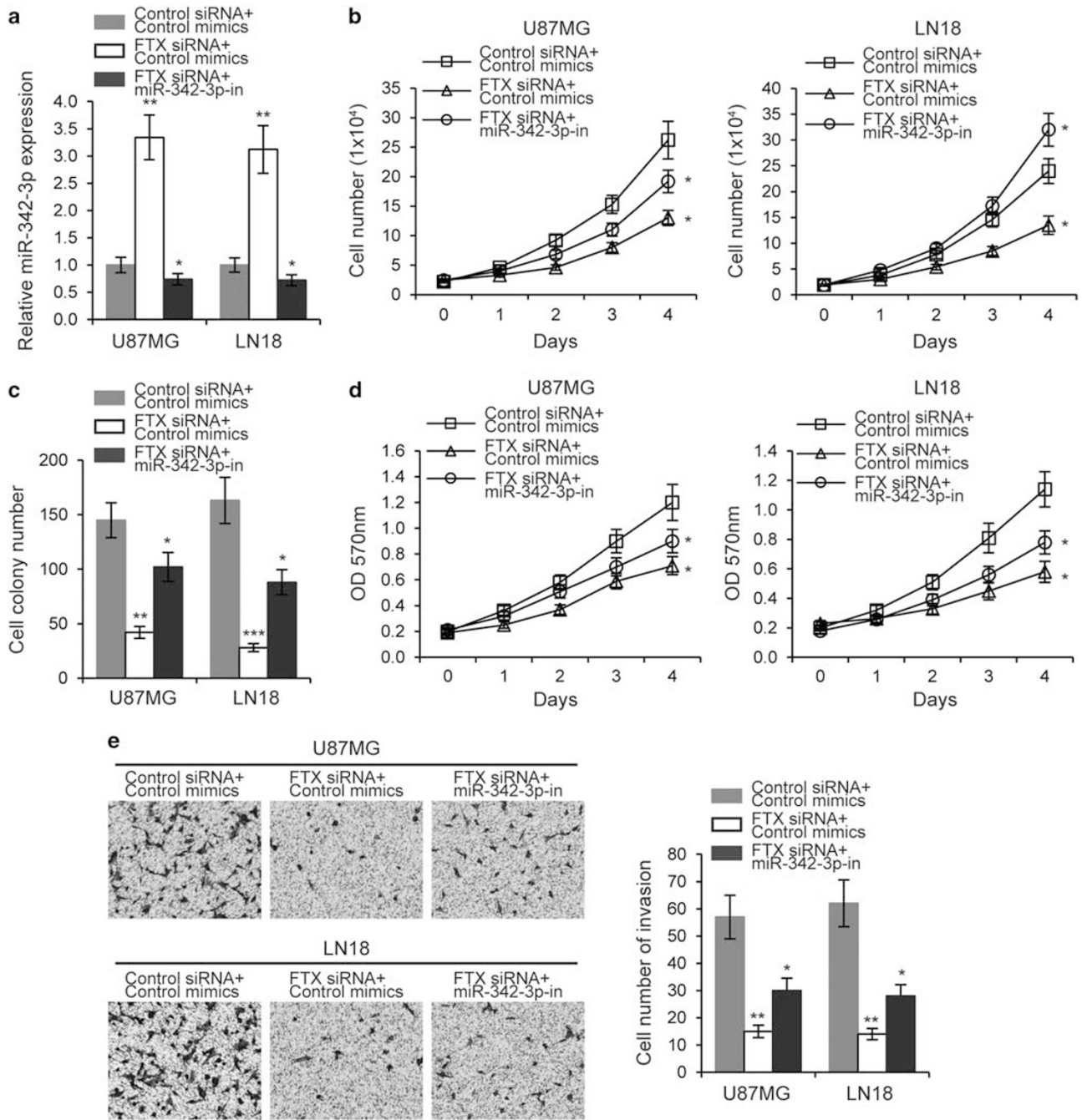


**Figure 5** Repression of miR-342-3p rescued FTX-induced glioma cell inhibition. (a) miR-342-3p expression was determined by qRT-PCR in U87MG and LN18 cells transfected with control small interfering RNA (siRNA)+control mimics, FTX siRNA+control mimics, or FTX siRNA+miR-342-3p-in. (b) Cell numbers; (c) colony formation; and (d) MTT (3-(4,5-dimethylthiazol-2-yl)-2,5-diphenyltetrazolium bromide) cell proliferation assays in U87MG and LN18 cells transfected with control siRNA+control mimics, FTX siRNA+control mimics, or FTX siRNA+miR-342-3p-in. (e) Transwell invasion assays in U87MG and LN18 cells transfected with control siRNA+control mimics, FTX siRNA+control mimics, or FTX siRNA+miR-342-3p-in (left). Quantification of invading cells (right). Data shown are the mean  $\pm$  s.d. of three independent experiments. \* $P < 0.05$ , \*\* $P < 0.01$  and \*\*\* $P < 0.001$ .

which subsequently activates p53 signaling.<sup>17,28</sup> Our findings indicate that FTX can serve as a biomarker for diagnosis of glioma. FTX suppresses proliferation and metastasis of hepatocellular carcinoma, and upregulation of FTX was associated with poorer overall survival in patients with

colorectal cancer. Taken together with previous studies, it is possible that FTX exerts different functions in cancers originating in different tissues, and may represent a novel therapeutic target for treatment of gliomas and hepatocellular carcinoma.



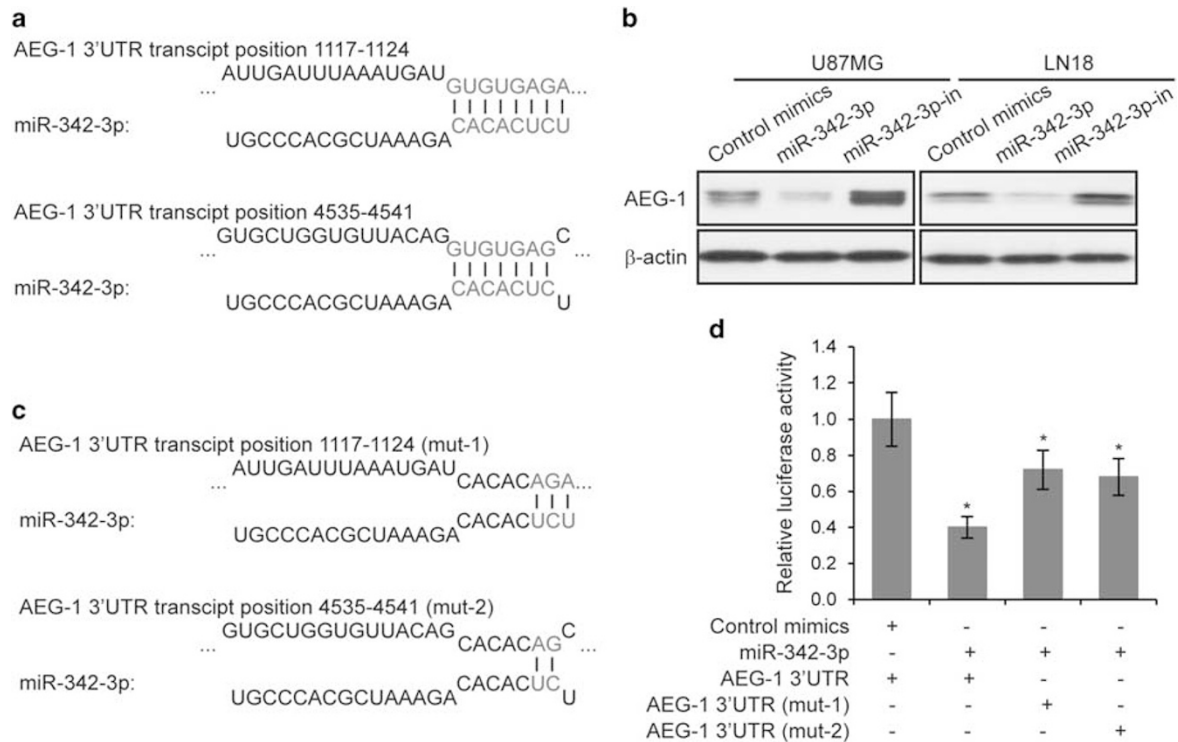


**Figure 6** miR-342-3p directly targeted astrocyte-elevated gene-1 (AEG-1). (a) Predicted miR-342-3p target sequences in the AEG-1 3'-untranslated region (3'-UTR). (b) Western blot analysis of AEG-1 expression in U87MG and LN18 cells transfected with control mimics miR-342-3p or miR-342-3p-in.  $\beta$ -Actin was used as a loading control. (c) Five common nucleotides of AEG-1 3'-UTR were mutated to prevent wide bonding with miR-342-3p. (d) HEK293T cells were transfected with AEG-1 3'-UTR wild-type or mutant reporter plasmids along with miR-342-3p, and then luciferase activity assays were performed. Data shown are the mean  $\pm$  s.d. of three independent experiments. \* $P < 0.05$ .

We found that the effects of FTX on proliferation and invasion of glioma cells was mediated by miR-342-3p. Expression of miR-342-3p was negatively correlated with FTX expression in different stages of gliomas in tissues. Depletion of FTX resulted in significant increases of miR-342-3p expression. Importantly, transfection with miR-342-3p-in partially rescued the reduced proliferation and invasion activities induced by knockdown of FTX. These results demonstrated an essential role for miR-342-3p in regulating proliferation and invasion of glioma cells as a direct target for FTX, and also indicated that FTX may have other important targets. The structure of lncRNAs may be complicated, containing several functional domains that can sense or bind other RNAs and proteins, and possibly DNA.<sup>8</sup> Regulation of gene expression by lncRNAs may take place at the epigenetic, transcriptional and post-transcriptional levels.<sup>29</sup> The other functions of FTX in glioma progression require further investigation.

Our findings also extend prior investigations by revealing that miR-342-3p directly targets AEG-1 in glioma cells. A previous study revealed specific expression of miRNAs in the peripheral blood of GM patients.<sup>30</sup> miR-342-3p was reported to inhibit tumorigenesis in several human cancers, including cervical,<sup>31</sup> hepatocellular,<sup>32</sup> lung,<sup>33,34</sup> and triple-negative breast cancer.<sup>35</sup> In this study, we found that

miR-342-3p directly regulated the expression of AEG-1 by targeting the 3'-UTR of AEG-1 mRNA. As suggested previously, AEG-1 may promote growth and epithelial-mesenchymal transition during glioma development.<sup>36,37</sup> Taken together, our findings revealed an essential role of the FTX in enhancing expression of AEG-1 via inhibition of miR-342-3p thereby promoting proliferation and invasion of glioma cells.

However, there are still several limitations in this study. Even though we showed that knockdown of FTX significantly inhibited proliferation and invasion of glioma cell lines, whether overexpression of FTX further enhances these processes remains to be investigated. In addition, because of the long-time cell culture in nutrient-rich media as plastic-adherent monolayers and the lack of supporting non-cancerous stroma, cell lines we used in this study may not represent the heterogeneity of tumors as they exist in patients.<sup>38</sup> And more efforts, especially *in vivo* studies, are still needed to determine the role of FTX in patient-derived cells or xenograft.

In conclusion, we found that expression of FTX and miR-342-3p is associated with progression of gliomas. FTX promotes proliferation and invasion of glioma cells by regulating miR-342-3p, which further directly targets AEG-1. FTX and miR-342-3p may serve as biomarkers of

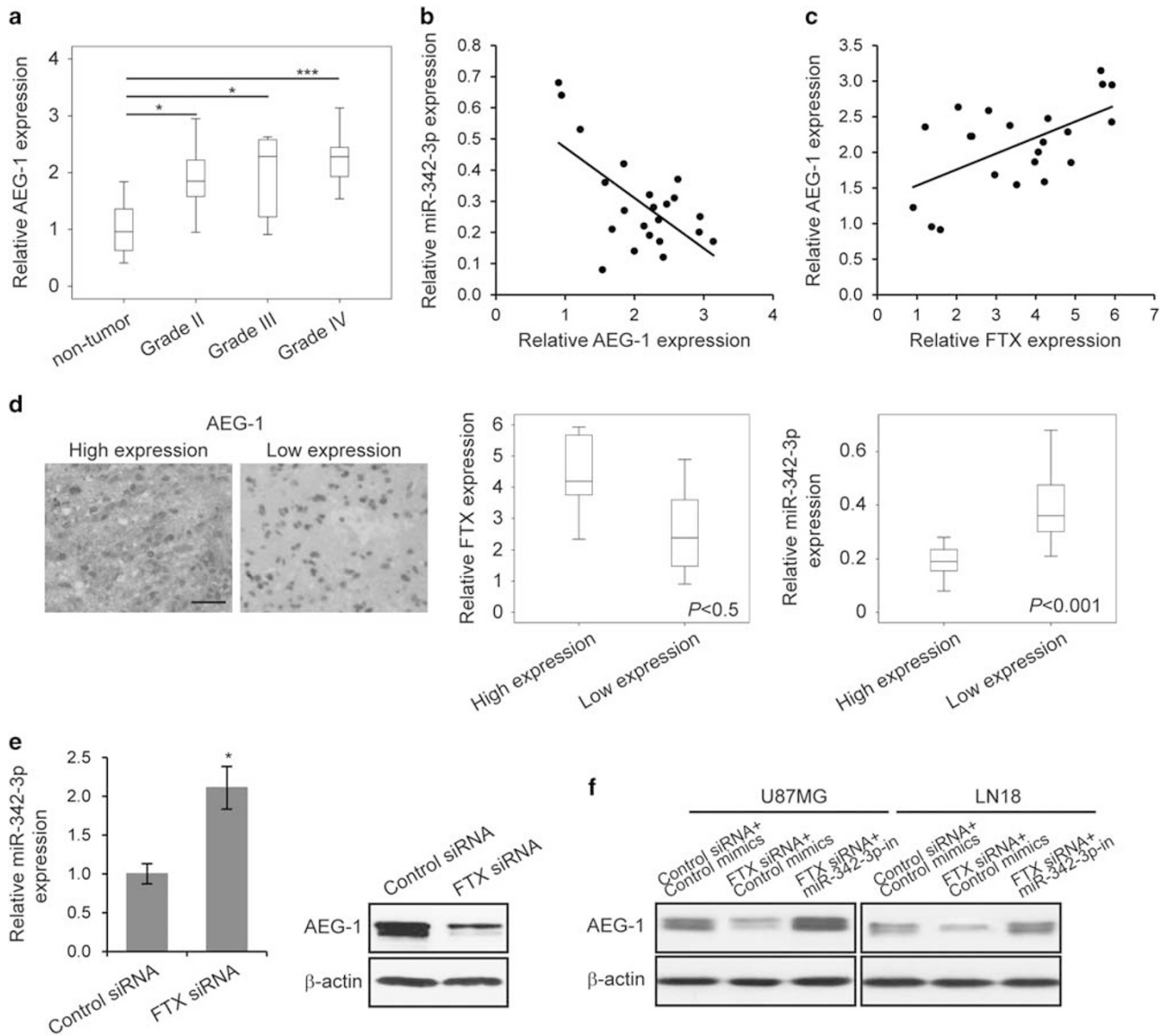


**Figure 7** FTX-regulated astrocyte-elevated gene-1 (AEG-1) expression through miR-342-3p. **(a)** AEG-1 expression was determined by qRT-PCR in 22 clinical glioma tissues. **(b)** Pearson’s correlation analysis between miR-342-3p and AEG-1 in 22 clinical glioma tissues;  $r = -0.629$ ,  $P < 0.001$ . **(c)** Pearson’s correlation analysis between AEG-1 and FTX in 22 clinical glioma tissues;  $r = -0.580$ ,  $P < 0.001$ . **(d)** Immunohistochemistry (IHC) stainings were performed of AEG-1 on glioma specimens and samples were separated to high and low expression groups based on the intensity of AEG-1 staining. The FTX and miR-342-3p expression were analyzed between high and low AEG-1 expression groups. Scale bar = 100  $\mu\text{m}$ . **(e)** miR-342-3p and AEG-1 expression were examined in subcutaneous tumors of FTX-knockdown and control groups by quantitative qRT-PCR and western blot, respectively. Data shown are the mean  $\pm$  s.d. of three independent experiments. \* $P < 0.05$ . **(f)** Western blot analysis for AEG-1 expression in U87MG and LN18 cells transfected with control siRNA+control mimics, FTX siRNA+control mimics, or FTX siRNA+miR-342-3p-in.

glioma diagnosis, and novel therapeutic targets for the treatment of gliomas.

**ACKNOWLEDGMENTS**

This study was supported by Heilongjiang Province Department of Education Grant (12541487) and Natural Science Foundation of Heilongjiang Province (H2016032).

**DISCLOSURE/CONFLICT OF INTEREST**

The authors declare no conflict of interest.

- Schwartzbaum JA, Fisher JL, Aldape KD, *et al*. Epidemiology and molecular pathology of glioma. *Nat Clin Pract Neurol* 2006;2: 494–503; quiz 491 p following 516.
- Ostrom QT, Bauchet L, Davis FG, *et al*. The epidemiology of glioma in adults: a ‘state of the science’ review. *Neuro-Oncology* 2014;16:896–913.
- Louis DN, Ohgaki H, Wiestler OD, *et al*. The 2007 WHO Classification of Tumours of the Central Nervous System. *Acta Neuropathol* 2007;114: 97–109.
- von Deimling A, Louis DN, Wiestler OD. Molecular pathways in the formation of gliomas. *Glia* 1995;15:11.
- Maleszewska M, Kaminska B. Is glioblastoma an epigenetic malignancy? *Cancers (Basel)* 2013;5:1120–1139.

6. Phillips HS, Kharbanda S, Chen R, *et al*. Molecular subclasses of high-grade glioma predict prognosis, delineate a pattern of disease progression, and resemble stages in neurogenesis. *Cancer Cell* 2006;9:157–173.
7. van den Boom J, Wolter M, Kuick R, *et al*. Characterization of gene expression profiles associated with glioma progression using oligonucleotide-based microarray analysis and real-time reverse transcription-polymerase chain reaction. *Am J Pathol* 2003;163:1033–1043.
8. Mercer TR, Mattick JS. Structure and function of long noncoding RNAs in epigenetic regulation. *Nat Struct Mol Biol* 2013;20:300–307.
9. Kapranov P, Cheng J, Dike S, *et al*. RNA maps reveal new RNA classes and a possible function for pervasive transcription. *Science* 2007;316:1484–1488.
10. Carninci P, Kasukawa T, Katayama S, *et al*. The transcriptional landscape of the mammalian genome. *Science* 2005;309:1559–1563.
11. Khalil AM, Guttman M, Huarte M, *et al*. Many human large intergenic noncoding RNAs associate with chromatin-modifying complexes and affect gene expression. *Proc Natl Acad Sci USA* 2009;106:11667–11672.
12. Wang KC, Chang HY. Molecular mechanisms of long noncoding RNAs. *Mol Cell* 2011;43:904–914.
13. Ng SY, Johnson R, Stanton LW. Human long non-coding RNAs promote pluripotency and neuronal differentiation by association with chromatin modifiers and transcription factors. *EMBO J* 2012;31:522–533.
14. Huarte M. The emerging role of lncRNAs in cancer. *Nat Med* 2015;21:1253–1261.
15. Kiang KM, Zhang XQ, Leung GK. Long non-coding RNAs: the key players in glioma pathogenesis. *Cancers (Basel)*. 2015;7:1406–1424.
16. Li R, Qian J, Wang YY, *et al*. Long noncoding RNA profiles reveal three molecular subtypes in glioma. *CNS Neurosci Ther* 2014;20:339–343.
17. Zhang X, Sun S, Pu JK, *et al*. Long non-coding RNA expression profiles predict clinical phenotypes in glioma. *Neurobiol Dis* 2012;48:1–8.
18. Chureau C, Chantalat S, Romito A, *et al*. Ftx is a non-coding RNA which affects Xist expression and chromatin structure within the X-inactivation center region. *Hum Mol Genet* 2011;20:705–718.
19. Liu F, Yuan JH, Huang JF, *et al*. Long noncoding RNA FTX inhibits hepatocellular carcinoma proliferation and metastasis by binding MCM2 and miR-374a. *Oncogene* 2016;35:5422–5434.
20. Zhang W, Shen C, Li C, *et al*. miR-577 inhibits glioblastoma tumor growth via the Wnt signaling pathway. *Mol Carcinogen* 2016;55:575–585.
21. Paraskevopoulou MD, Vlachos IS, Karagkouni D, *et al*. DIANA-LncBase v2: indexing microRNA targets on non-coding transcripts. *Nucleic Acids Res* 2016;44:D231–D238.
22. Agarwal V, Bell GW, Nam JW, *et al*. Predicting effective microRNA target sites in mammalian mRNAs. *Elife* 2015; 4.
23. Shi X, Wang X. The role of MTDH/AEG-1 in the progression of cancer. *Int J Clin Exp Med* 2015;8:4795–4807.
24. Norden AD, Wen PY. Glioma therapy in adults. *Neurologist* 2006;12:279–292.
25. Karipidis KK, Benke G, Sim MR, *et al*. Occupational exposure to ionizing and non-ionizing radiation and risk of glioma. *Occup Med* 2007;57:518–524.
26. Hatanpaa KJ, Burma S, Zhao D, *et al*. Epidermal growth factor receptor in glioma: signal transduction, neuropathology, imaging, and radioresistance. *Neoplasia (New York, NY)* 2010;12:675–684.
27. Zhang J-X, Han L, Bao Z-S, *et al*. HOTAIR, a cell cycle-associated long noncoding RNA and a strong predictor of survival, is preferentially expressed in classical and mesenchymal glioma. *Neuro-Oncology* 2013;15:1595–1603.
28. Wang P, Ren Z, Sun P. Overexpression of the long non-coding RNA MEG3 impairs in vitro glioma cell proliferation. *J Cell Biochem* 2012;113:1868–1874.
29. Kornienko AE, Guenzl PM, Barlow DP, *et al*. Gene regulation by the act of long non-coding RNA transcription. *BMC Biol* 2013;11:1–14.
30. Dong L, Li Y, Han C, *et al*. miRNA microarray reveals specific expression in the peripheral blood of glioblastoma patients. *Int J Oncol* 2014;45:746–756.
31. Li XR, Chu HJ, Lv T, *et al*. miR-342-3p suppresses proliferation, migration and invasion by targeting FOXM1 in human cervical cancer. *FEBS Lett* 2014;588:3298–3307.
32. Zhao L, Zhang Y. miR-342-3p affects hepatocellular carcinoma cell proliferation via regulating NF-kappaB pathway. *Biochem Biophys Res Commun* 2015;457:370–377.
33. Xie X, Liu H, Wang M, *et al*. miR-342-3p targets RAP2B to suppress proliferation and invasion of non-small cell lung cancer cells. *Tumour Biol* 2015;36:5031–5038.
34. Tai MC, Kajino T, Nakatochi M, *et al*. miR-342-3p regulates MYC transcriptional activity via direct repression of E2F1 in human lung cancer. *Carcinogenesis* 2015;36:1464–1473.
35. Ma T, Zhang J, Wu J, *et al*. Effect of miR-342-3p on chemotherapy sensitivity in triple-negative breast cancer. *Zhong Nan Da Xue Xue Bao Yi Xue Ban* 2014;39:488–495.
36. Lee SG, Kim K, Kegelman TP, *et al*. Oncogene AEG-1 promotes glioma-induced neurodegeneration by increasing glutamate excitotoxicity. *Cancer Res* 2011;71:6514–6523.
37. Zou M, Zhu W, Wang L, *et al*. AEG-1/MTDH-activated autophagy enhances human malignant glioma susceptibility to TGF- $\beta$ 1-triggered epithelial-mesenchymal transition. *Oncotarget* 2016;7:13122–13138.
38. Williams SA, Anderson WC, Santaguida MT, *et al*. Patient-derived xenografts, the cancer stem cell paradigm, and cancer pathobiology in the 21st century. *Lab Invest* 2013;93:970–982.